

# A Numerical Simulation of Diffusion-Convection Problems in Heterogeneous Media with a Point Source

(Simulasi Berangka Masalah Resapan-Perolakan dalam Media Heterogen dengan Punca Titik)

IMAM SOLEKHUDIN<sup>1,\*</sup>, NOORMA YULIA MEGAWATI<sup>1</sup>, SOLIKHATUN<sup>1</sup>, INDIRA ANGGRIANI<sup>1,2</sup>, MOHAMMAD IVAN AZIS<sup>3</sup>,  
IKHA MAGDALENA<sup>4</sup> & WIDOWATI<sup>5</sup>

<sup>1</sup>Department of Mathematics, Faculty of Mathematics and Natural Sciences, Universitas Gadjah Mada, Yogyakarta 55281, Indonesia

<sup>2</sup>Institut Teknologi Kalimantan, Balikpapan, Kalimantan Timur 76127, Indonesia

<sup>3</sup>Department of Mathematics, Faculty of Mathematics and Natural Sciences, Universitas Hasanuddin, Makassar 90245, Indonesia

<sup>4</sup>Faculty of Mathematics and Natural Sciences, Bandung Institute of Technology, Bandung 40132, Indonesia

<sup>5</sup>Department of Mathematics, Faculty of Science and Mathematics, Universitas Diponegoro, Semarang 50275, Indonesia

*Received: 3 December 2024/Accepted: 18 July 2025*

## ABSTRACT

In this paper, some time-independent diffusion-convection problems in anisotropic media are considered. To study the problems, the governing equation of the problems is transformed into a diffusion-convection equation in a homogeneous isotropic media. The transformed equation with respect to transformed boundary conditions are solved numerically using Dual Reciprocity Boundary Element Method (DRBEM). The method is tested using several problems involving time-independent diffusion-convection. Two of the problems are with analytical solution, and the other problems are with point sources without known analytical solution.

Keywords: Anisotropic media; DRBEM; point source; time-independent diffusion-convection

## ABSTRAK

Dalam makalah ini, beberapa masalah resapan-konveksi bebas masa dalam media anisotropik dipertimbangkan. Untuk mengkaji masalah, persamaan yang mengawal masalah diubah menjadi persamaan resapan-konveksi dalam media homogen isotropik. Persamaan berkenaan dengan keadaan sempadan yang diubah diselesaikan secara berangka menggunakan Kaedah Unsur Dual Kesalingan Sempadan (DRBEM). Kaedah ini diuji menggunakan beberapa masalah yang melibatkan resapan-konveksi bebas masa. Dua daripada masalah adalah dengan penyelesaian analitik dan masalah lain adalah dengan sumber mata tanpa penyelesaian analitik yang diketahui.

Kata kunci: DRBEM; media anisotropik; resapan-konveksi bebas masa; sumber mata

## INTRODUCTION

Diffusion-convection challenges have long captivated researchers. Numerous studies have explored these topics, including those by Capinski et al. (1999), Huxtable et al. (2004), Norris et al. (2003), and Paddock and Eesley (1986). Paddock and Eesley (1986) investigated transient thermorefectance in thin metal films. Capinski et al. (1999) focused on measuring thermal conductivity using a picosecond optical pump and probe technique. Norris et al. (2003) applied femtosecond pump-probe methods to analyze certain materials, and Huxtable et al. (2004) conducted thermal conductivity imaging at a micrometer scale. The majority of these studies are experimental in nature.

One approach to studying diffusion-convection in anisotropic materials is through mathematical modeling. However, analytical solutions are typically not possible for the resulting mathematical model. Thus, this paper employs a numerical solution using a type of Boundary Element Method (BEM) known as the Dual Reciprocity Boundary Element Method (DRBEM). A key advantage of these methods is their capability to reduce the dimensionality of the problem. The time-independent, two-dimensional spatial problems examined here can be reduced to one-dimensional problems. Many researchers have used boundary element methods in their studies (Ashar & Solekhudin 2021; Clements & Lobo 2010; Munadi et al. 2020, 2019; Solekhudin 2018). For instance, Clements and

Lobo (2010), Munadi et al. (2019, 2020), Solekhdin, Sari and Makhrus (2024), and Solekhdin et al. (2018) applied boundary element techniques to analyze water infiltration in homogeneous soils, while Ashar and Solekhdin (2021) employed this method to simulate substance dispersion from a point source in a river.

Researchers have primarily focused on problems in homogeneous materials. However, some studies have applied boundary element techniques to nonhomogeneous materials as well. For example, Solekhdin (2020) used the method to solve infiltration problems in layered soils, while Ang and Clements (2009) applied it to the nonlinear heat equation in nonhomogeneous anisotropic materials. Additionally, Azis et al. (2021) utilized the technique to address issues in anisotropic functionally graded materials.

This study extends the work of Ashar and Solekhdin (2021), in which the fluid was assumed to be homogeneous. In the present paper, we address the effects of fluid heterogeneity. Specifically, we investigate time-dependent diffusion-convection problems in a heterogeneous fluid with a point source. As in the previous study, the DRBEM is employed to solve the problems. To evaluate the accuracy of the method, two test cases with known analytical solutions are created. Subsequently, the method is applied to time-independent diffusion-convection problems involving a point source, for which no analytical solutions are available.

#### PROBLEM FORMULATION

In this study, we investigate fluid flow through a straight channel that has a width of one unit. At one boundary of the flow domain, there is a discharge pipe that releases a substance, such as a pollutant, into the flow. The geometry of the problem is illustrated in Figure 1.

The fluid is assumed to be heterogeneous, with no flux across the boundary. It is further assumed that, beyond a certain downstream distance from the pipe, the concentration of the substance becomes uniform (the flux is zero). Based on these assumptions, this research examines the influence of fluid heterogeneity, convection coefficients, and quantity of the substance source on the distribution of the substance within the fluid.

#### MATHEMATICAL MODEL AND NUMERICAL SOLUTION METHOD

In this section, the mathematical model of steady diffusion-convection problems in anisotropic media with a point source is presented. A brief derivation of DRBEM for solving the problems is also presented. The general form of diffusion-convection equation is (Atangana 2018)

$$\frac{\partial u}{\partial t} = \nabla \cdot (D \nabla u - \mathbf{v}u) + g, \quad (1)$$

where  $u$  is the substance concentration;  $D$  is the diffusivity;  $\mathbf{v}$  is the velocity with which the substance moving; and  $g$  is the source or sink term. In this study, it is assumed that no chemical reactions affect the quantity of the substance, so the function  $g$  depends solely on space. For steady two-dimensional diffusion-convection in heterogeneous media, Equation (1) can be written as

$$k_{11}u_{xx} + (k_{12} + k_{21})u_{xy} + k_{22}u_{yy} - v_1u_x - v_2u_y + g(x,y) = 0. \quad (2)$$

Here  $[k_{ij}]$  is the diffusivity, and  $\mathbf{v} = [v_1, v_2]$ , where  $v_1$  and  $v_2$  are components of fluid velocity vector in  $x$  and  $y$  direction respectively.

In problems involving a point source located at  $(a, b)$ , where the total substance released from the source is given by  $Q(x, y) = Q(a, b)$ , the source term  $g$  can be written as

$$g(x, y) = Q(x, y) \delta(x, y; a, b)$$

where  $Q$  represents the source intensity and  $\delta$  denotes the Dirac delta function. The delta function is defined as

$$\delta(x, y; a, b) = \begin{cases} 0, & (x, y) \neq (a, b) \\ \infty, & (x, y) = (a, b) \end{cases},$$

and satisfies the property

$$\int_{-\infty}^{\infty} \int_{-\infty}^{\infty} Q(x, y) \delta(x, y; a, b) dx dy = \int_{b-\epsilon}^{b+\epsilon} \int_{a-\epsilon}^{a+\epsilon} Q(x, y) \delta(x, y; a, b) dx dy = Q(a, b),$$

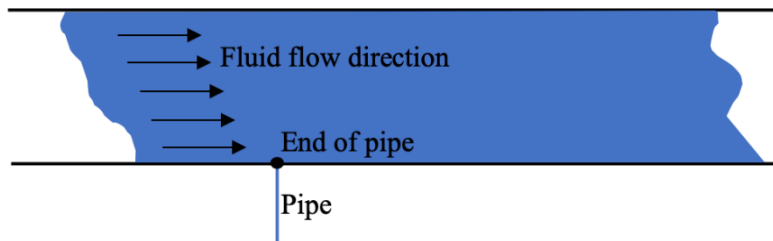


FIGURE 1. Geometrical setup of the problem in this study

for any  $\epsilon > 0$ . This representation captures the assumption that the source is concentrated at a single point  $(a, b)$ , with no contribution elsewhere, and that the total quantity of substance introduced into the fluid equals  $Q(a, b)$ , consistent with the modelling framework.

The problem described in the preceding section has the following domain

$$\Omega = \{(x, y) : x \in \mathbb{R} \text{ and } 0 < y < 1\}.$$

To implement the Dual Reciprocity Boundary Element Method (DRBEM), it is necessary to have imposed boundaries such that the domain is enclosed by a simple closed curve. For this purpose, the values of  $x$  must lie within an interval  $[\alpha, \beta]$ , where  $\alpha, \beta \in \mathbb{R}$ . The source point is taken to be  $(1, 0)$ . Through a series of trial-and-error computational experiments, the interval  $[\alpha, \beta] = [0, 5]$  was identified as appropriate, as it ensures that the imposed boundary does not affect significantly on the solution at interior points. Now, the new domain is

$$\Omega' = \{(x, y) : 0 < x < 5 \text{ and } 0 < y < 1\},$$

bounded by a simple closed curve  $T'$ . Hence, the boundary conditions for the diffusion-convection problems described in the preceding section are

$$u = 0, x = 0 \text{ and } 0 < y < 1, \quad (3)$$

$$v = 0, 0 < x < 5 \text{ and } y = 0, \quad (4)$$

$$v = 0, x = 5 \text{ and } 0 < y < 1, \quad (5)$$

$$v = 0, 0 < x < 5 \text{ and } y = 1, \quad (6)$$

where  $v = \sum_{j=1}^2 \sum_{i=1}^2 k_{ij} \frac{\partial u}{\partial x_i} n_{x_j}$  is the flux. Here  $x_1 = x$  and  $x_2 = y$ , and  $n = [n_x, n_y]$  is the normal vector pointing out region  $\Omega'$ .

The DRBEM cannot be applied to solve Equation (3) due to the inequality  $k_{11} \neq k_{22}$  and the presence of the  $u_{xy}$  term. Therefore, it is necessary to transform the coordinate system into a new one through a set of transformations, as outlined by Pramesthi, Solekhuudin and Azis (2021). A summary of the set of transformations is provided below; for more comprehensive details, please refer to Pramesthi, Solekhuudin and Azis (2021).

Let

$$K = \begin{bmatrix} k_{11} & k_{12} \\ k_{21} & k_{22} \end{bmatrix}.$$

Making use of rotation

$$\begin{bmatrix} x' \\ y' \end{bmatrix} = \begin{bmatrix} p & q \\ -q & p \end{bmatrix} \begin{bmatrix} x \\ y \end{bmatrix},$$

and dilatation

$$X = x' \left( \frac{\lambda}{k_1} \right)^{1/2} ; \quad Y = y' \left( \frac{\lambda}{k_2} \right)^{1/2},$$

Equation (1) can be transformed into

$$u_{xx} + u_{yy} - V_1 u_x - V_2 u_y + G(X, Y) = 0, \quad (7)$$

where

$$V_1 = (v_1 p + v_2 q) \left( \frac{1}{\lambda k_1} \right)^{1/2}, \quad V_2 = (v_2 p - v_1 q) \left( \frac{1}{\lambda k_2} \right)^{1/2},$$

$p$  and  $q$  satisfy  $p^2 + q^2 = 1$ ,

$$\begin{bmatrix} p & -q \\ q & p \end{bmatrix} \begin{bmatrix} k_1 & 0 \\ 0 & k_2 \end{bmatrix} = \begin{bmatrix} k_{11} & k_{12} \\ k_{21} & k_{22} \end{bmatrix} \begin{bmatrix} p & -q \\ q & p \end{bmatrix},$$

and

$$\begin{aligned} G(X, Y) &= g \left( p \left( \frac{k_1}{\lambda} \right)^{\frac{1}{2}} X - q \left( \frac{k_2}{\lambda} \right)^{\frac{1}{2}} Y, q \left( \frac{k_1}{\lambda} \right)^{\frac{1}{2}} X + p \left( \frac{k_2}{\lambda} \right)^{\frac{1}{2}} Y \right) \\ &= q \left( p \left( \frac{k_1}{\lambda} \right)^{\frac{1}{2}} X - q \left( \frac{k_2}{\lambda} \right)^{\frac{1}{2}} Y, q \left( \frac{k_1}{\lambda} \right)^{\frac{1}{2}} X + p \left( \frac{k_2}{\lambda} \right)^{\frac{1}{2}} Y \right) \\ &\quad \times \delta \left( p \left( \frac{k_1}{\lambda} \right)^{\frac{1}{2}} X - q \left( \frac{k_2}{\lambda} \right)^{\frac{1}{2}} Y, q \left( \frac{k_1}{\lambda} \right)^{\frac{1}{2}} X + p \left( \frac{k_2}{\lambda} \right)^{\frac{1}{2}} Y; a, b \right). \end{aligned}$$

Here  $k_1$  and  $k_2$  are the eigenvalues of matrix  $K$ . Moreover, domain  $\Omega'$ , boundary  $T'$ , and Boundary conditions (3) to (6) are also transformed using the same transformations. Let the transformed domain and boundary are denoted by  $\Omega^*$  and  $T^*$ , respectively.

Now, we solve the diffusion-convection with a point source modelled in Equation (7), with respect to the transformations of Boundary conditions (2) – (5) using the DRBEM. To implement the DRBEM, using Gauss's theorem, we can express the solution of Equation (7) in an integral equation. The integral equation is

$$\begin{aligned} \lambda(\xi, \eta) u(\xi, \eta) &= \int_{T^*} [u(X, Y) \frac{\partial \Psi}{\partial n}(X, Y; \xi, \eta) - \Psi(X, Y; \xi, \eta) \frac{\partial u}{\partial n}(X, Y)] ds \\ &\quad + \iint_{\Omega^*} \Psi(X, Y; \xi, \eta) [V_1 u_x + V_2 u_y] dXdY - \Psi(a, b; \xi, \eta) Q(a, b), \end{aligned} \quad (8)$$

where  $T^*$  and  $\Omega^*$  are the transformations of  $T'$  and  $\Omega'$ , respectively,  $\Psi(X, Y; \xi, \eta)$  is the fundamental solution of Laplace equation, and

$$\lambda(\xi, \eta) = \begin{cases} 1, & (\xi, \eta) \in \Omega^* \\ \frac{1}{2}, & (\xi, \eta) \text{ on smooth part of } T^* \end{cases}.$$

The DRBEM is formulated based on Integral Equation (8). The implementation of the DRBEM proceeds as follows:

#### Boundary Discretization

The boundary  $T^*$  is discretized into  $N$  connected line segments, denoted by  $C^{(n)}$ ,  $n = 1, 2, \dots, N$ .

#### Collocation Points

For each boundary segment, the midpoint is selected as a collocation point. Additionally,  $L$  interior collocation points are chosen within the domain. In total, there are  $N+L$  collocation points, denoted as  $(a^{(k)}, b^{(k)})$ , for  $k = 1, 2, \dots, N+L$ .

#### Function Approximations

The values of  $u$  and its normal derivative  $\frac{\partial u}{\partial n}$  on each segment are approximated by:

$$(u(x, y) \approx u(a^{(k)}, b^{(k)}) = u^{(k)},$$

and

$$\frac{\partial u}{\partial n}(x, y) \approx \left. \frac{\partial u}{\partial n} \right|_{(x, y) = (a^{(k)}, b^{(k)})} = u_n^{(k)}.$$

#### Formulation of the System of Linear Equations

Substituting these approximations into the integral equation (8), and evaluating the solution at the collocation points,  $(\xi, \eta) = (a^{(n)}, b^{(n)})$ , the problem is reduced to a system of linear equations of the form:

$$\lambda^{(n)} u^{(n)} = \sum_{k=1}^N [\mathcal{F}_2^{(nk)} u^{(k)} - \mathcal{F}_1^{(nk)} u_n^{(k)}] + \sum_{k=1}^{N+L} \mu^{(nk)} [V_1 u_x^{(k)} + V_2 u_y^{(k)}] - \Psi(a, b; \xi, \eta) Q(a, b), \quad n = 1, 2, \dots, N+L.$$

The terms involved in this formulation are defined as follows (Ang 2007):

$$\mathcal{F}_1^{(nk)} = \int_{C^{(k)}} \Psi(X, Y; a^{(k)}, b^{(k)}) ds, \quad \mathcal{F}_2^{(nk)} = \int_{C^{(k)}} \frac{\partial \Psi}{\partial n}(X, Y; a^{(k)}, b^{(k)}) ds,$$

and

$$\mu^{(nk)} = \sum_{m=1}^{N+L} \Gamma^{(nm)} \omega^{(mk)}.$$

Here

$$\Gamma^{(nm)} = \lambda^{(n)} X^{(nm)} + \sum_{k=1}^N [\mathcal{F}_1^{(nk)} X_n^{(nk)} - \mathcal{F}_2^{(nk)} X^{(nk)}],$$

$\omega^{(mk)}$  is defined by

$$\sum_{k=1}^{N+L} \omega^{(mk)} \rho^{(kn)} = \begin{cases} 1, & \text{if } m = n \\ 0, & \text{if } m \neq n \end{cases},$$

$$\rho^{(kn)} = 1 + \frac{(a^{(k)} - a^{(n)})^2 + (b^{(k)} - b^{(n)})^2}{\left[ \sqrt{(a^{(k)} - a^{(n)})^2 + (b^{(k)} - b^{(n)})^2} \right]^3},$$

and

$$X^{(kn)} = \frac{1}{4} \left[ (a^{(k)} - a^{(n)})^2 + (b^{(k)} - b^{(n)})^2 \right] + \frac{1}{16} \left[ (a^{(k)} - a^{(n)})^2 + (b^{(k)} - b^{(n)})^2 \right]^2 + \frac{1}{4} \left[ \sqrt{(a^{(k)} - a^{(n)})^2 + (b^{(k)} - b^{(n)})^2} \right]^5.$$

#### Solution of the System of Linear Equations

The resulting system is solved to obtain the values of  $u$  at the collocation points.

### RESULTS AND DISCUSSION

In this section, the DRBEM is applied to solve diffusion-convection problems with a point source in heterogeneous media. Initially, the DRBEM is used to solve two diffusion-convection problems with known analytical solutions. This implementation aims to evaluate the method's accuracy and efficiency. Subsequently, the DRBEM is employed to solve a variety of diffusion-convection problems with a point source in heterogeneous fluid flows.

#### PROBLEMS WITH KNOWN ANALYTICAL SOLUTIONS

We consider two problems with known analytical solutions. The two problems are as follows. *Problem 1*

The first problem considers a diffusion-convection governed by the partial differential equation

$$2u_{xx} + 2u_{xy} - 3u_{yy} + 10u_x + 4u_y = 0, \quad (8)$$

subject to the following Dirichlet boundary conditions:

$$u = \exp(-x), \quad 0 < x < 1 \text{ and } y = 0, \quad (9)$$

$$u = \exp(-1 - 2y), \quad x = 1 \text{ and } 0 < y < 1, \quad (10)$$

$$u = \exp(-x - 2), \quad 0 < x < 1 \text{ and } y = 1, \quad (11)$$

$$u = \exp(-2y), \quad x = 0 \text{ and } 0 < y < 1. \quad (12)$$

The analytic solution to this boundary value problem is given by

$$u = \exp(-x - 2y). \quad (13)$$

TABLE 1. Numerical vs analytical results obtained using 20 segments and 80 segments at selected points

Point	Numerical results		Analytical results	Absolute errors	
	20 Segments	80 Segments		20 Segments	80 Segments
(0.1,0.1)	0.74656665	0.74083991	0.74081822	0.00574843	0.00002169
(0.5,0.1)	0.49798653	0.49660038	0.49658530	0.00140122	0.00001507
(0.9,0.1)	0.33444177	0.33291510	0.33287108	0.00157068	0.00004401
(0.1,0.5)	0.33473802	0.33293328	0.33287108	0.00186693	0.00006220
(0.5,0.5)	0.22333456	0.22315852	0.22313016	0.00020440	0.00002836
(0.9,0.5)	0.15112736	0.14957991	0.14956862	0.00155874	0.00001130
(0.1,0.9)	0.15422081	0.14963251	0.14956862	0.00465219	0.00006389
(0.5,0.9)	0.10133543	0.10030410	0.10025884	0.00107659	0.00004525
(0.9,0.9)	0.07201250	0.06726116	0.06720551	0.00480698	0.00005564

To solve this problem, the DRBEM is implemented using 361 interior collocation points. Two different sets of line segments are considered: 20 segments and 80 segments. Some of the results are summarized in Table 1.

Table 1 shows that the DRBEM yields more accurate results when 80 boundary segments are used, compared to the results obtained with only 20 segments. This observation indicates that increasing the number of boundary segments enhances the accuracy of the numerical solution. Furthermore, the numerical results show good agreement with the corresponding analytical solution, confirming the reliability of the method.

#### Problem 2

In this problem, a diffusion-convection problem with a source term is governed by

$$9u_{xx} + 4u_{xy} - 3u_{yy} + 9u_x + 4u_y + 3\pi^2 \exp(-x) \sin(\pi y) = 0, \quad (14)$$

with boundary conditions as follows.

$$v = -3\pi \exp(-x), \quad 0 < x < 1 \text{ and } y = 0, \quad (15)$$

$$u = \exp(-1) \sin(\pi y), \quad x = 1 \text{ and } 0 < y < 1, \quad (16)$$

$$u = 0, \quad 0 < x < 1 \text{ and } y = 1, \quad (17)$$

$$v = 9 \sin(\pi y), \quad x = 0 \text{ and } 0 < y < 1. \quad (18)$$

The analytic solution of Problem 2 is

$$u = \exp(-x) \sin(\pi y). \quad (19)$$

To solve Problem 2 as that in Problem 1, 361 interior collocation points are used. Four segment configurations are considered: 40, 80, 120, and 160 segments. Some of the results obtained are presented in Figure 2.

Let  $E$  be the absolute error of the numerical solution obtained. Figure 2 illustrates the graphs of  $\log(E)$  obtained by implementing the DRBEM with 361 interior points with

four different numbers of segment. Specifically: Figure 2(a) shows  $\log(E)$  at  $x = 0.2$ , Figure 2(b) at  $x = 0.4$ , Figure 2(c) at  $x = 0.6$ , Figure 2(d) at  $x = 0.8$ . Figure 2 presents the numerical error and solution comparison for a 2D simulation problem at four different lines along the  $y$ -axis. Subplots (a) through (d) illustrate the logarithmic absolute error,  $\log(E)$ , of the numerical solution with respect to the analytical solution for different values of  $x = 0.2, 0.4, 0.6$ , and  $0.8$ , respectively. Four different boundary discretization are evaluated:  $N = 40, 80, 120$ , and  $160$ .

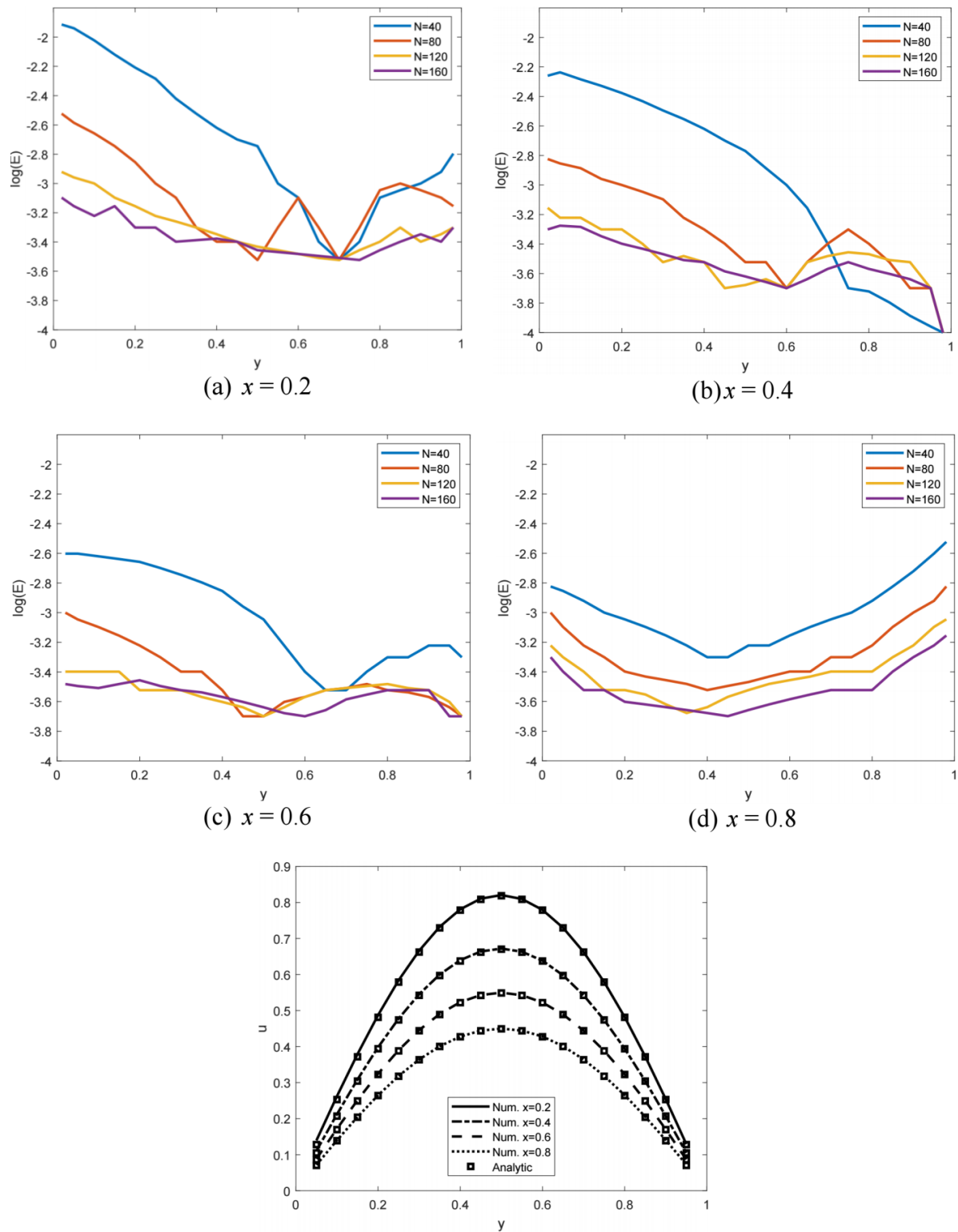
Across all subplots, it can be observed that the numerical error decreases as the segment or element increases (i.e., higher  $N$ ). For instance, in each subfigure, the curve corresponding to  $N = 40$  results in the highest error, while  $N = 160$  shows the lowest. This behaviour confirms that the numerical method employed is convergent, and increasing the number of segments improves accuracy.

Subfigure (e) compares the numerical solutions at different values of  $x$ ,  $x = 0.2, 0.4, 0.6$ , and  $0.8$  for a fixed number of segments,  $N = 40$  with the analytical solution (represented by square markers). As can be observed, the numerical results relatively close to the analytical solutions, suggesting that even at a relatively small number of segments, the numerical scheme shows a good accuracy. These findings affirm that DRBEM is an effective numerical approach for addressing diffusion-convection problems of this type.

#### PROBLEMS WITH UNKNOWN ANALYTICAL SOLUTIONS

In this section, we examine the spread of substances originating from a point source within the laminar flow of a heterogeneous fluid along the  $x$ -axis (where  $v_2 = 0$ ). The mathematical formulation of these problems is represented by the equation:

$$k_{11}u_{xx} + (k_{12} + k_{21})u_{xy} + k_{22}u_{yy} - v_1u_x + Q(x,y) \delta(x,y; 1,0) = 0, \quad (20)$$



(e) Analytical (square) vs numerical solutions with  $N = 40$ .

FIGURE 2. Absolute errors resulted from various line segments at selected values of  $x$  and comparison of numerical vs analytical solutions



subject to the boundary conditions outlined in Equations (2) through (5). Four distinct problem scenarios are explored in this section. Before delving into the four cases, it is essential to determine the number of elements required to implement the DRBEM effectively, ensuring a balance between accuracy and computational efficiency. For this purpose, we examine the substance dispersion problem governed by the equation:

$$9u_{xx} + 4u_{xy} + 3u_{yy} - 2u_x + 2\delta(x, y; 1, 0) = 0, \quad (21)$$

subject to boundary conditions given in Equations (3) to (6). In this analysis, 931 interior collocation points are used. We explore six different element ( $N$ ) configurations: 60, 120, 180, 240, 300, and 360. The DRBEM is implemented using MATLAB R2018b with these segment configurations. Table 2 summarizes the computational time associated with running the numerical simulations. As the problem lacks an analytical solution, we define a quantity  $\delta(x, y)$  as follows:

$$\delta(x, y) = |u(x, y) - u_{360}(x, y)|, \quad (22)$$

where  $u(x, y)$  represents the numerical solution at  $(x, y)$  obtained using the specified number of segments, and  $u_{360}(x, y)$  is the numerical solution at  $(x, y)$  computed with 360 segments. Selected values of  $\delta$  are displayed in Figure 3.

Figure 3 illustrates the values of  $\delta$  within the domain. Specifically, Figure 3(a) presents  $\delta$  values at five distinct points along  $x = 1$ , Figure 3(b) shows values at  $x = 3$ , and Figure 3(c) displays values at  $x = 4.5$ . Figure 3(d) shows surface plots of  $\delta$ . From the figure, it is evident that  $\delta$  increases as  $x$  becomes larger. Additionally, as  $N$  increases, the values of  $\delta$  decrease. Notably, for  $N = 240$ , the  $\delta$  values are relatively small or close to zero. Based on these results,  $N = 240$  is selected for implementing the DRBEM to solve the subsequent problems.

#### Problem Set 1

In this set, the diffusivity coefficients are defined as  $k_{11} = 9$ ,  $k_{12} = 2$ , and  $k_{22} = 3$ . The focus is on examining the effects of fluid velocity and the amount of substances emitted from the source on substance dispersion. Two values of  $v_1$  are considered:  $v_1 = 1$  and  $v_1 = 2$ . Additionally, two different values of  $Q(x, y)$  are examined:  $Q(x, y) = 1$  and  $Q(x, y) = 2$ .

#### Problem Set 2

In this set, the diffusivity coefficients are fixed at  $k_{11} = 9$  and  $k_{22} = 3$ , while the flow velocity is set to  $v_1 = 2$ , and the source quantity is  $Q(x, y) = 2$ . The diffusivity  $k_{12}$  is varied, with three values being analyzed:  $k_{12} = 1$ ,  $k_{12} = 2$ , and  $k_{12} = 3$ . The purpose of varying  $k_{12}$  is to analyze the effect of  $k_{12}$  to the values of  $u$ . Selected numerical solutions from both Problem Set 1 and Problem Set 2 are depicted in Figure 4.

Figure 4(a) presents the numerical results from Problem Set 1, where four scenarios are analyzed. The

first scenario examines substance dispersion with a source quantity of  $Q(x, y) = 2$  in a homogeneous fluid characterized by flow velocity  $v_1 = 2$  and diffusivity coefficients of 4.8. In the other three scenarios, the diffusivity coefficients are set as  $k_{11} = 9$ ,  $k_{12} = 2$ , and  $k_{22} = 3$ . In the second scenario, we set  $v_1 = 2$  and  $Q(x, y) = 2$ . The third scenario uses  $v_1 = 2$  and  $Q(x, y) = 1$ . The fourth scenario considers  $v_1 = 1$  and  $Q(x, y) = 2$ .

It can be seen that at smaller values of  $y$ , the highest concentration of substance occurs at  $x = 1$ , which is the point of source located. The results indicate that substance dispersion is higher in a homogeneous fluid. This suggests that lower horizontal diffusivity ( $k_{11}$ ) leads to increased substance accumulation. This finding aligns with real-world observations: when substances are continuously released into a medium with low diffusivity, the slower dispersion causes higher substance concentrations over time compared to a medium with higher diffusivity, which allows faster spread.

Among the three cases with heterogeneous fluids, the scenario with  $v_1 = 1$  exhibits the highest substance concentration, which is expected because the slower horizontal flow results in reduced dispersion. Conversely, the scenario with  $v_1 = 2$  and  $Q(x, y) = 1$  has the lowest substance concentration. This can be attributed to the reduced amount of substances being released, which is half that of the other cases.

Figure 4(b) displays graphs of  $u$  along the  $x$ -axis at selected  $y$ -values for the case where  $k_{11} = 9$  and  $k_{22} = 3$ , with three different values of  $k_{12}$ . In this scenario, the flow velocity is  $v_1 = 2$  and the substance source quantity is  $Q(x, y) = 2$ . The results indicate that an increase in  $k_{12}$  leads to higher substance distribution.

#### Problem Set 3

In this analysis, the diffusivity coefficients  $k_{12} = 2$  and  $k_{22} = 3$  are held constant, while the flow velocity is set to  $v_1 = 2$ , and the source term is  $Q(x, y) = 2$ . The diffusivity  $k_{11}$  is varied, taking the values  $k_{11} = 7$ ,  $k_{11} = 9$ , and  $k_{11} = 11$ . The objective is to study how changes in  $k_{11}$  affect the distribution of  $u$ .

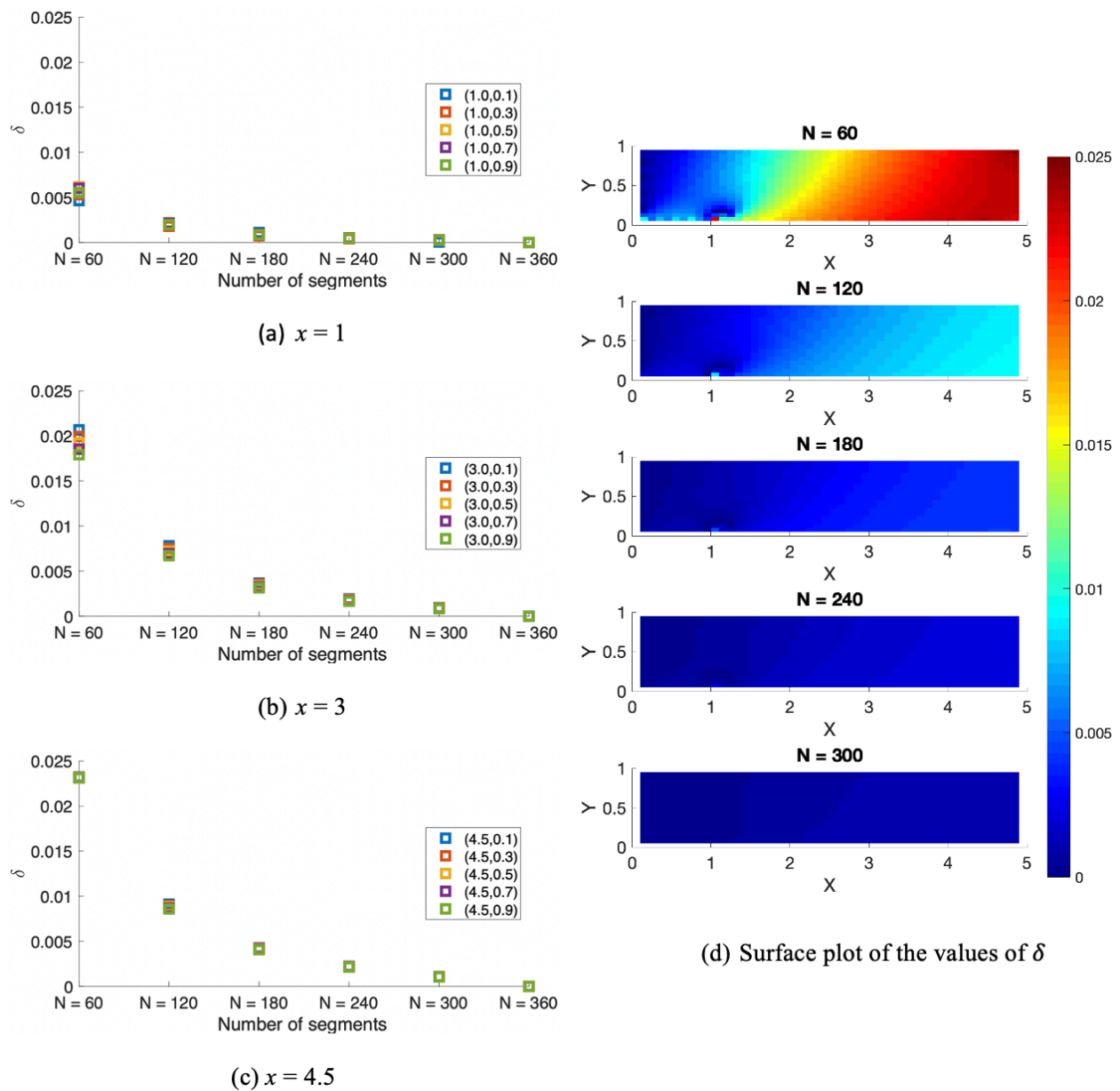
#### Problem Set 4

Here, the diffusivity coefficients  $k_{11} = 9$  and  $k_{12} = 2$  are fixed, with the flow velocity set to  $v_1 = 2$ , and the source term defined as  $Q(x, y) = 2$ . The diffusivity  $k_{22}$  is varied, analyzing the values  $k_{22} = 1$ ,  $k_{22} = 3$ , and  $k_{22} = 5$ . This variation aims to examine the influence of  $k_{22}$  on the distribution of  $u$ . Selected numerical results from Problem Set 3 and Problem Set 4 are illustrated in Figure 5.

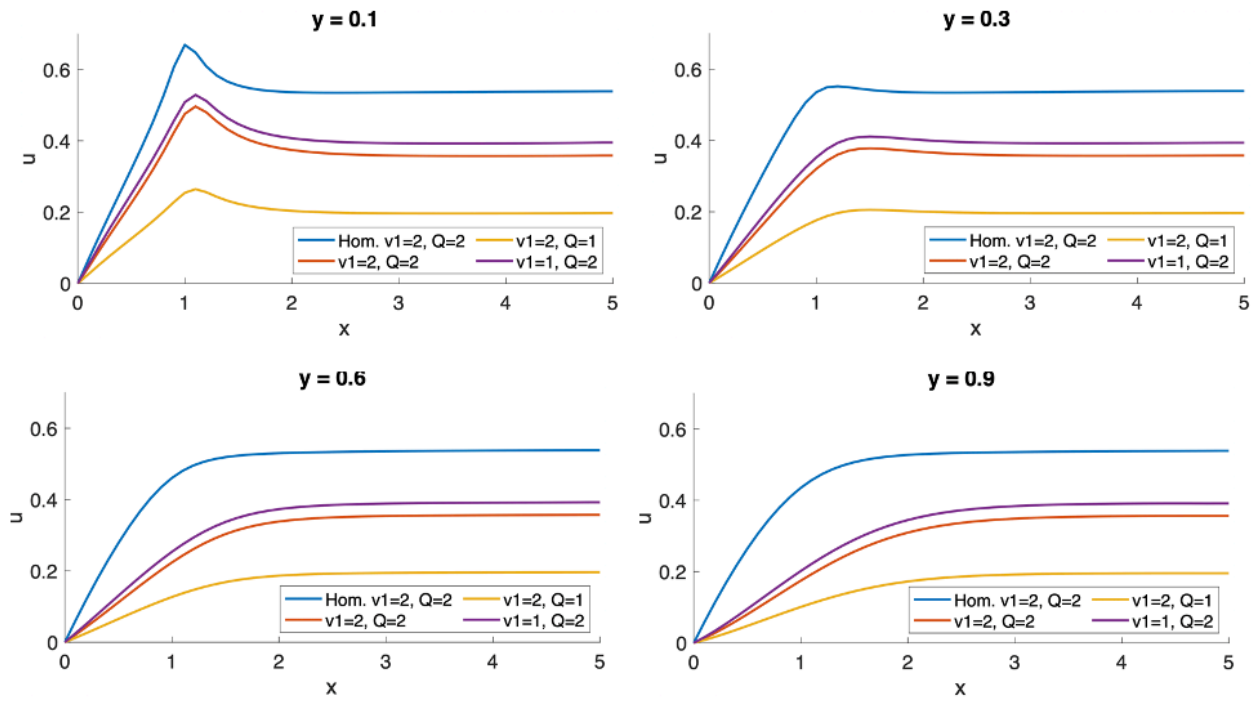
Figure 5(a) displays numerical results from Problem Set 3. The diffusivity coefficients are  $k_{22} = k_{11} = 2$  and  $k_{22} = 3$ , with the source term  $Q(x, y) = 2$  and flow velocity  $v_1 = 2$ . Three scenarios are analyzed: the first considers  $k_{11} = 9$ , the second uses  $k_{11} = 7$ , and the third employs  $k_{11} = 11$ . For all scenarios, four fixed  $y$ -values are examined:  $y = 0.1$ ,  $y = 0.3$ ,  $y = 0.6$ , and  $y = 0.9$ . The aim is to evaluate

TABLE 2. Computational time needed for running the code for implementing the DRBEM

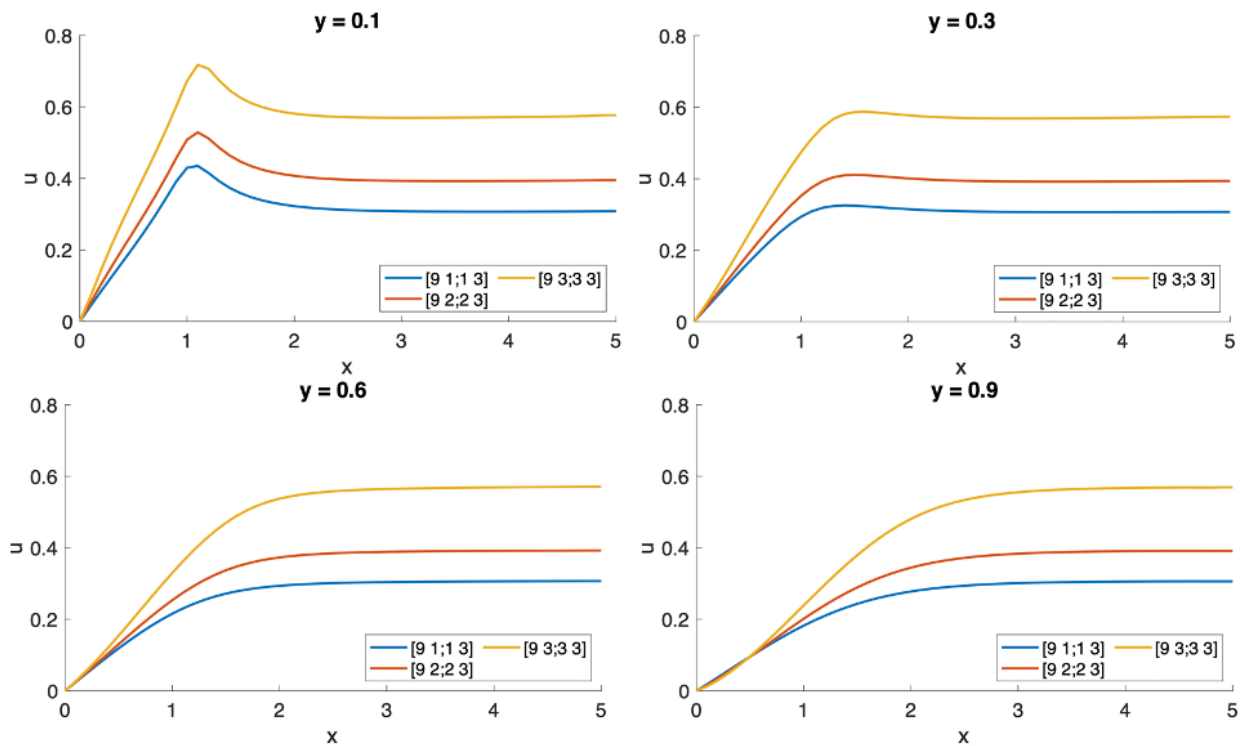
Number of segments	Computational time (s)
60	55.047675
120	107.576988
180	178.185288
240	247.787502
300	339.073585
360	400.235451

FIGURE 3. Values of  $\delta$  at selected absolute errors resulted from various line segments at selected values of  $x$  and comparison numerical vs analytical solutions



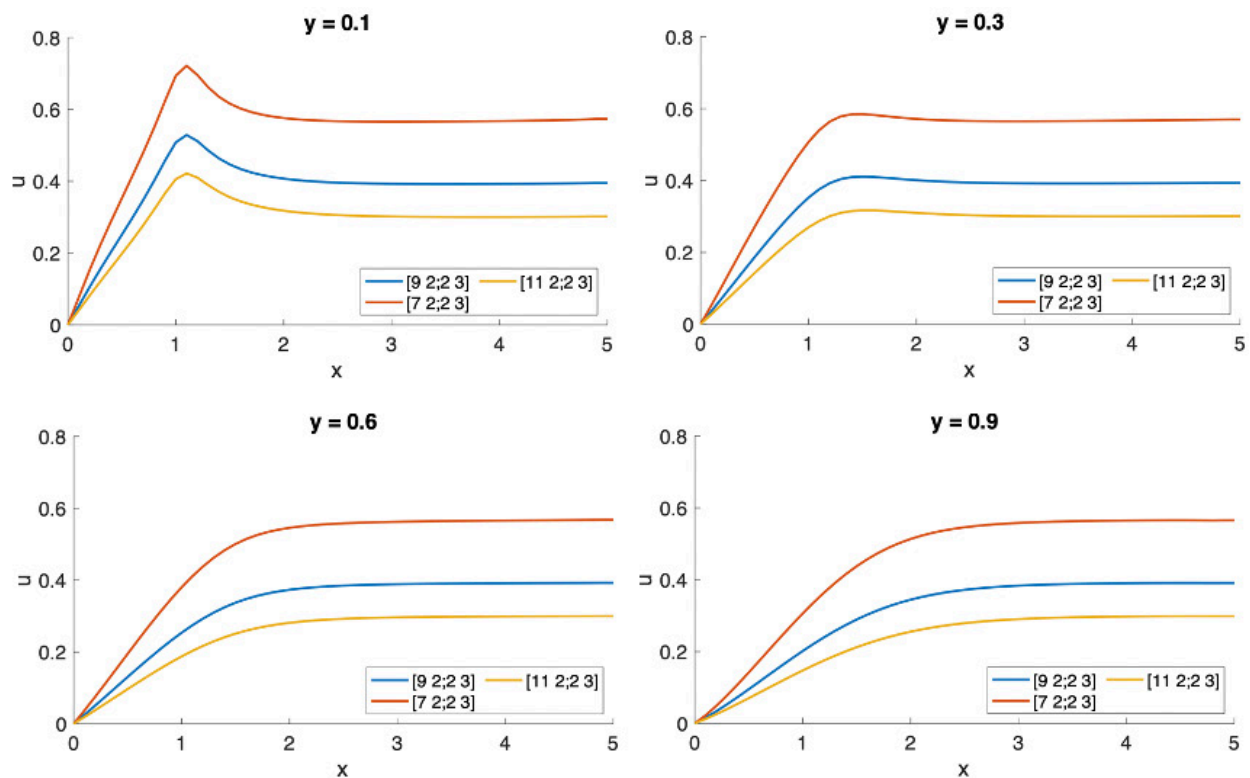
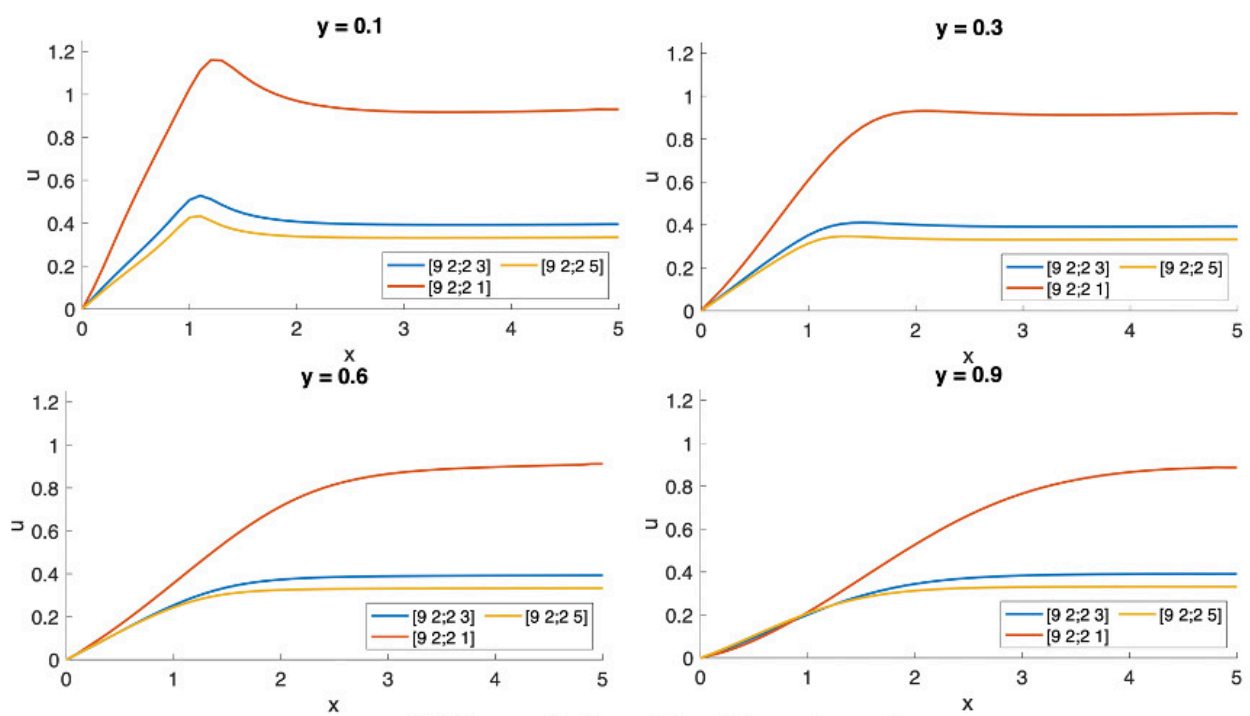


(a) Cases with  $k_{11} = 9, k_{12} = k_{21} = 2$  and  $k_{22} = 3$ .



(b) Cases with different values of  $k_{12}$

FIGURE 4. Graphs of  $u$  at selected values of  $y$  for Problem set 1 and Problem set 2

(a) Cases with  $k_{12} = k_{21} = 2$  and  $k_{22} = 3$ .(b) Cases with  $k_{11} = 9$  and  $k_{12} = k_{21} = 2$ .FIGURE 5. Graphs of  $u$  at selected values of  $y$  along  $x$ -axis for Problem set 3 and Problem set 4

how variations in  $k_{11}$ , horizontal diffusivity, influence the substance distribution in fluid. It is evident that higher horizontal diffusivity reduces substance concentration, which aligns with expectations: faster spreading results in lower concentrations.

Figure 5(b) illustrates graphs of  $u$  along the  $x$ -axis for the same  $y$ -values as in Figure 5(a), focusing on the scenario where  $k_{11} = 9$  and  $k_{12} = k_{21} = 2$ . Here, three different values of  $k_{22}$  are considered. The flow velocity remains  $v_1 = 2$ , and the source term is  $Q(x, y) = 2$ . The objective is to observe the effect of vertical diffusivity on substance distribution in fluid. The results show that increasing  $k_{22}$  leads to lower substance concentrations, similar to the patterns observed in Figure 5(a). Higher diffusivity values enhance spreading, which in turn decreases concentration levels in the fluid. The distribution of substance concentration in the fluid for all cases is represented as surface plots in Figure 6.

#### CONCLUDING REMARKS

The Dual Reciprocity Boundary Element Method (DRBEM) is used to solve diffusion-convection problems involving the spread of substances from a point source in a flowing heterogeneous fluid. Initially, the method is applied to two problems with known analytical solutions to validate its accuracy. Following this, it is used for solving substance spread problems where analytical solutions are unavailable.

In cases with known analytical solutions, the results show that increasing the number of boundary elements improves accuracy. However, this also increases computational time. For the substance spread problems in flowing heterogeneous fluid, the DRBEM is applied under various conditions. In one scenario, the diffusion coefficients are fixed, and the fluid flow velocity and the quantity of substance entering the fluid are varied. Another

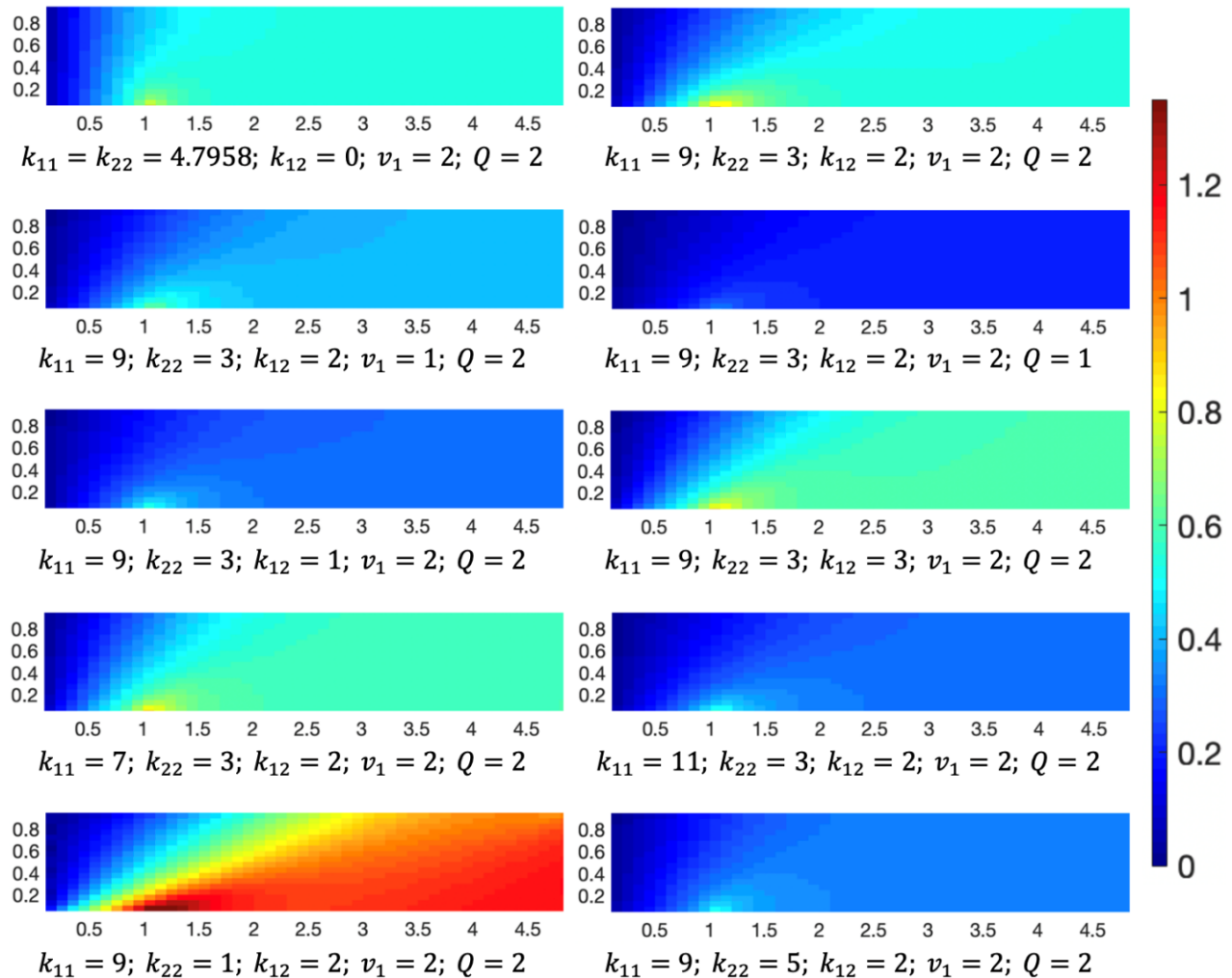


FIGURE 6. Surface plots of  $u$  for all problems analysed in this study

scenario involves fixing the flow velocity, the substance quantity, and the diffusion coefficients, except for the horizontal diffusion coefficient, which is varied. A similar scenario considers varying the values of  $k_{12}$ . In a further scenario, all parameters are fixed except  $k_{22}$ , which are varied.

The results show that lower fluid flow velocities lead to higher substance concentrations in the fluid. Similarly, lower horizontal and vertical diffusion coefficients result in higher concentrations. However, decreasing  $k_{12}$  leads to lower concentrations. Additionally, increasing vertical diffusion coefficients is more effective at reducing substance concentrations compared to horizontal diffusion coefficients.

#### ACKNOWLEDGEMENTS

We acknowledge the financial support from Program KATALIS 2024 (Grant No. 3767/UNI/DITLIT/PT.01.03/2024) and RKI 2025 (Grant No. 1593/UNI/DITLIT/Dit-Lit/PT.01.03/2025).

#### REFERENCES

- Ang, W.T. 2007. *A Beginner's Course in Boundary Element Methods*. Florida: Universal Publishers.
- Ang, W.T. & Clements, D.L. 2009. Nonlinear heat equation for nonhomogeneous anisotropic materials: A dual-reciprocity boundary element solution. *Numerical Methods for Partial Differential Equations* 26: 771-784.
- Ashar, N.Y. & Solekhuudin, I. 2021. A numerical study of steady pollutant spread in water from a point source. *Engineering Letters* 29(3): 840-848.
- Atangana, A. 2018. *Fractional Operators with Constant and Variable Order with Application to Geo-Hydrology*. Massachusetts: Academic Press.
- Azis, M.I., Solekhuudin, I., Aswad, M.H., Hamzah, S. & Jalil, A.R. 2021. A combined laplace transform and boundary element method for unsteady laplace problems of several classes of anisotropic functionally graded materials. *Engineering Letters* 29: 534-542.
- Capinski, W.S., Maris, H.J., Ruf, T., Cardona, M., Ploog, K. & Katzer, D.S. 1999. Thermal-conductivity measurements of GaAs/AlAs superlattices using a picosecond optical pump-and-probe technique. *Phys. Rev. B* 59(12): 8105-8113.
- Clements, D.L. & Lobo, M. 2010. A BEM for time dependent infiltration from an irrigation channel. *Engineering Analysis with Boundary Elements* 34: 1100-1104.
- Huxtable, S., Cahill, D.G., Fauconnier, V., White, J.O. & Zhao, J.C. 2004. Thermal conductivity imaging at micrometre-scale resolution for combinatorial studies of materials. *Nature Mater.* 3: 298-301.
- Munadi, Solekhuudin, I., Sumardi & Zulijanto, A. 2020. A numerical study of steady infiltration from a single irrigation channel with an impermeable soil layer. *Engineering Letters* 28(3): 1-8.
- Munadi, Solekhuudin, I., Sumardi & Zulijanto, A. 2019. Steady water flow from different types of single irrigation channel. *JP Journal of Heat and Mass Transfer* 16(1): 95-106.
- Norris, P.M., Caffrey, A.P., Stevens, R.J., Klopff, J.M., James, J., McLeskey, T. & Smith, A.N. 2003. Femtosecond pump-probe nondestructive examination of materials. *Rev. Sci. Instrum.* 74(1): 400-406.
- Paddock, C.A. & Eesley, G.L. 1986. Transient thermos reflectance from thin metal films. *J. Appl. Phys.* 60(1): 285-290.
- Pramesthi, A.A.N., Solekhuudin, I. & Azis, M.I. 2021. Implementation of dual reciprocity boundary element method for heat conduction problems in anisotropic solid. *IAENG International Journal of Applied Mathematics* 52(1): 122-130.
- Solekhuudin, I. 2020. Boundary interface water infiltration into layered soils using dual reciprocity methods. *Engineering Analysis with Boundary Elements* 119: 280-292.
- Solekhuudin, I. 2018. A numerical method for time-dependent infiltration from periodic trapezoidal channels with different types of root-water uptake. *IAENG International Journal of Applied Mathematics* 48(1): 84-89.
- Solekhuudin, I., Sari, A.K & Makhrus, F. 2024. An iterative dual reciprocity method for a class of infiltration problems in two-layered soils with different types of root-water uptake. *IAENG International Journal of Applied Mathematics* 54(7): 1390-1399.
- Solekhuudin, I., Purnama, D., Malysa, N.H. & Sumardi. 2018. Characteristic of water flow in heterogeneous soils. *JP Journal of Heat and Mass Transform* 15(3): 597-608.

\*Corresponding author; email: imams@ugm.ac.id